

Suppression and Overexpression of Adenosylhomocysteine Hydrolase-like Protein 1 (AHCYL1) Influences Zebrafish Embryo Development

A POSSIBLE ROLE FOR AHCYL1 IN INOSITOL PHOSPHOLIPID SIGNALING*

Received for publication, March 17, 2006, and in revised form, June 2, 2006. Published, JBC Papers in Press, June 5, 2006, DOI 10.1074/jbc.M602520200

Benjamin J. Cooper[‡], Brian Key[§], Adrian Carter[§], Nicola Z. Angel[‡], Derek N. J. Hart^{‡¶}, and Masato Kato^{‡1}

From the [‡]Dendritic Cell Program, Mater Medical Research Institute, Brisbane, Queensland 4101, Australia and [§]Discipline of Anatomy and Developmental Biology, School of Biomedical Sciences, University of Queensland, Brisbane, Queensland 4172, Australia, and the [¶]School of Medicine, University of Queensland, Herston, Queensland 4006, Australia

Adenosylhomocysteine hydrolase-like protein 1 (AHCYL1) is a novel intracellular protein with ~50% protein identity to adenosylhomocysteine hydrolase (AHCY), an important enzyme for metabolizing *S*-adenosyl-L-homocysteine, the by-product of *S*-adenosyl-L-homomethionine-dependent methylation. AHCYL1 binds to the inositol 1,4,5-trisphosphate receptor, suggesting that AHCYL1 is involved in intracellular calcium release. We identified two zebrafish AHCYL1 orthologs (zAHCYL1A and -B) by bioinformatics and reverse transcription-PCR. Unlike the ubiquitously present AHCY genes, AHCYL1 genes were only detected in segmented animals, and AHCYL1 proteins were highly conserved among species. Phylogenetic analysis suggested that the AHCYL1 gene diverged early from AHCY and evolved independently. Quantitative reverse transcription-PCR showed that zAHCYL1A and -B mRNA expression was regulated differently from the other AHCY-like protein zAHCYL2 and zAHCY during zebrafish embryogenesis. Injection of morpholino antisense oligonucleotides against zAHCYL1A and -B into zebrafish embryos inhibited zAHCYL1A and -B mRNA translation specifically and induced ventralized morphologies. Conversely, human and zebrafish AHCYL1A mRNA injection into zebrafish embryos induced dorsalized morphologies that were similar to those obtained by depleting intracellular calcium with thapsigargin. Human AHCY mRNA injection showed little effect on the embryos. These data suggest that AHCYL1 has a different function from AHCY and plays an important role in embryogenesis by modulating inositol 1,4,5-trisphosphate receptor function for the intracellular calcium release.

We discovered human adenosylhomocysteine hydrolase-like protein 1 (hAHCYL1²; previously termed dendritic cell-ex-

pressed AHCY-like protein, or DCAL) by differential display from the Hodgkin disease-derived cell line L428 (1). The hAHCYL1 protein (~60 kDa, 530 amino acids) consists of a novel N-terminal hydrophilic domain (106 amino acids) and a C-terminal domain (424 amino acids), which is homologous (51% protein identity) to the methylation pathway enzyme, AHCY (EC 3.3.1.1, ~46 kDa). AHCY is the evolutionarily conserved and ubiquitously expressed enzyme that catalyzes the reversible hydrolysis of *S*-adenosyl-L-homocysteine, a byproduct of the *S*-adenosyl-L-homomethionine-dependent methyltransferase reaction, into adenosine and homocysteine using NAD⁺ as a cofactor (2). Although AHCYL1 conserves the cysteines required for a tight globular structure of AHCY and the NAD⁺ binding motif, AHCYL1 lacks some binding sites for *S*-adenosyl-L-homocysteine, suggesting that AHCYL1 has a different function from AHCY. The N-terminal hydrophilic domain contains 79 polar or charged amino acids, including a cluster of Ser, Thr, and Tyr (potential phosphorylation sites), and this domain is likely to regulate AHCYL1 function (1).

AHCYL1 is highly conserved among species, and the human and mouse orthologs have 100% protein identity, suggesting a highly conserved function yet to be understood. The other AHCY-like protein KIAA0828 (termed AHCYL2 hereafter) has similar gene and protein structure to those of AHCYL1, but again its function is unknown (1, 3). In blood, hAHCYL1 mRNA was predominantly expressed in dendritic cells (DC), the most potent antigen-presenting cells for eliciting immune responses (4, 5), but not in other leukocytes. Increased hAHCYL1 mRNA expression during DC differentiation and activation suggested that hAHCYL1 plays a role in DC differentiation and function (1). However, the UniGene data base analysis (UniGene cluster Hs.4113) and our multiple tissue expression array analysis³ indicated that hAHCYL1 is also expressed in nonhematopoietic tissues, especially at high levels in neuronal and renal tissues.

Recently, Ando *et al.* (6) showed that AHCYL1 is identical to

* This work was supported by research grants from Pfizer and Mater Medical Research Institute. The costs of publication of this article were defrayed in part by the payment of page charges. This article must therefore be hereby marked "advertisement" in accordance with 18 U.S.C. Section 1734 solely to indicate this fact.

The nucleotide sequence(s) reported in this paper has been submitted to the GenBank™/EBI Data Bank with accession number(s) AY611473 (zAHCYL1A), AY611474 (zAHCYL1B), BK005364 (*fugu* fish AHCYL1), BK005417 (hAHCYL1B), and BK005418 (hAHCYL1C).

¹ To whom correspondence should be addressed: Mater Medical Research Institute, Aubigny Pl., South Brisbane, Queensland 4101, Australia. Tel.: 61-7-3840-2555; Fax: 61-7-3840-2550; E-mail: mkato@mmri.mater.org.au.

² The abbreviations used are: hAHCYL, human AHCYL; zAHCYL, zebrafish AHCYL; AHCYL, adenosylhomocysteine hydrolase-like protein; AHCY,

adenosylhomocysteine hydrolase; zAHCY, zebrafish AHCY; hAHCY, human AHCY; DC, dendritic cells; EGFP, enhanced green fluorescent protein; EST, expressed sequence tag; GAPDH, glyceraldehyde-3-phosphate dehydrogenase; hpf, hours postfertilization; IP₃, inositol 1,4,5-trisphosphate; IP₃R, inositol 1,4,5-trisphosphate receptor; RACE, rapid amplification of cDNA ends; RT, reverse transcription; E1–E20, exon 1–20, respectively.

³ B. J. Cooper, unpublished results.

an inositol 1,4,5-trisphosphate receptor (IP₃R)-binding protein (termed IP₃R-binding protein released with inositol 1,4,5-trisphosphate, or IRBIT). Binding of AHCYL1 to IP₃R, an important regulator of intracellular Ca²⁺ release, is mediated by its N-terminal domain, and its phosphorylation appears to be essential for the AHCYL1 binding. Importantly, the AHCYL1 binding site on IP₃R also mediates the IP₃-IP₃R interaction, suggesting that AHCYL1 regulates IP₃ binding to the IP₃R. The consequence of AHCYL1 interacting with the IP₃R remains to be elucidated, but it is of significant interest given the important regulating role other molecules (and other signaling pathways) have on Ca²⁺ as a result of IP₃R activation.

To investigate the function of AHCYL1, we chose the zebrafish (*Danio rerio*) as a model organism for molecular genetic analysis. We describe the cDNA cloning and genomic organization of the zAHCYL1, compare them with those of hAHCYL1 and other AHCYL1 homologs, and demonstrate the effect of suppression and overexpression of AHCYL1 on zebrafish development.

EXPERIMENTAL PROCEDURES

In Silico Cloning of zAHCYL1—Expressed sequence tags (ESTs) corresponding to zAHCYL1 were identified in the dbEST data base from the National Center for Biotechnology Information (NCBI) by performing a BLASTn search using hAHCYL1 coding sequence as the query. Nine overlapping ESTs (GenBankTM accession numbers CA473816, BI473660, BI885096, CD284541, BI430354, BI884776, BI473380, CD594351, and BF937243) were compiled using Sequencher software (Gene Codes, Ann Arbor, MI) to form a putative zAHCYL1 cDNA sequence. This sequence was used to design primers for cloning the full-length zAHCYL1 cDNA (described below). Exon/intron boundaries were determined via a zebrafish genomic BLAST search available from the Ensembl Zebrafish Genome Server.

Identification of AHCYL1 in Other Species—AHCYL1 orthologs in other species were identified by tBLASTn searches using hAHCYL1 protein sequence for enquiry on the NCBI genomic or EST data bases. Searches were conducted in the following organisms (data base used is shown in parentheses): *Anopheles gambiae* (genome), *Caenorhabditis elegans* (genome), *Drosophila melanogaster* (genome), *Takifugu rubripes* (genome), *Gallus gallus* (EST), *Plasmodium falciparum* (genome), *Saccharomyces cerevisiae* (genome), *Xenopus laevis* (EST), and the microbial genome data base (completed genomes only). To confirm that output sequences were AHCYL family orthologs and not AHCY orthologs, the sequences were assessed for (i) N-terminal domain containing conserved Ser/Thr residues and (ii) alignment with the hAHCY protein using NCBI pairwise BLAST indicating less similarity to hAHCY than hAHCYL1. Phylogenetic analysis was performed using the programs ClustalW for multiple sequence alignment and ProtDist for computing the phylogenetic tree and bootstrap values with 100 bootstrap cycles. Both programs are available on the Australian National Genomic Information Service Bioinformatics service (ANGIS; available on the World Wide Web at www.angis.org.au). The protein sequences included were

AHCYL1 orthologs from human (GenBankTM accession number AF315687), zebrafish (GenBankTM accession number AY611473, this report), fugu fish (GenBankTM accession number BK005364; this report), and fruit fly (GenBankTM accession number NM_139489 and NM_206499); AHCYL2 orthologs from human (GenBankTM accession number NM_015328) and zebrafish (GenBankTM accession number NM_201340); and AHCY orthologs from human (GenBankTM accession number NM_000687), mouse (GenBankTM accession number BC086781), zebrafish (GenBankTM accession number BC044200), and fruit fly (GenBankTM accession number NM_078609).

Prediction of Phosphorylation Sites and NAD⁺ Binding Domain—Potential Ser/Thr/Tyr phosphorylation sites in the AHCYL1 protein sequences were assessed using the program NetPhos 2.0 (7) on the ExPASy Molecular Biology server (available on the World Wide Web at au.expasy.org). The AHCY NAD⁺ binding region of the AHCYL1 proteins was defined using the Conserved Domain Database through NCBI.

RT-PCR Cloning of zAHCYL1—Total RNA was isolated from adult zebrafish head extracted with Trizol (Invitrogen) and 5'-rapid amplification of cDNA ends (RACE) for zAHCYL1 using the FirstChoice RLM RACE kit (Ambion, Austin, TX) carried out according to the manufacturer's instructions. First strand cDNA synthesis was carried out using 10 µg of the total RNA, and the primary PCR was performed using the outer adaptor primer (5'-GCTGATGGCGATGAATGAACACTG-3') and the gene-specific outer primer MK279 (5'-GCTGAGCTGTAGCTGTCCGTA-3', nucleotides 508–528 of zAHCYL1A) using AmpliTaq Gold (Applied Biosystems, Scoresby, Victoria, Australia). The primary PCR product was further amplified using the inner adaptor primer (5'-CGCGGATCCGAACACTGCGTTTGCTGGCTTTGATG-3') and the gene-specific inner primer MK280 (5'-TCCTGTTTGTCCTCCTGGTT-3', nucleotides 425–444 of zAHCYL1A) (see Fig. 1). The PCR was performed on a PTC 200 thermal cycler (MJ Research, Waltham, MA) with the following reaction cycle: 94 °C for 10 min; 35 cycles of 94 °C for 30 s, 58 °C for 30 s, and 72 °C for 30 s; 72 °C for 10 min.

Cloning of full-length zAHCYL1 coding sequence was performed using a Thermoscript RT-PCR system (Invitrogen). Briefly, 1 µg of total RNA from adult zebrafish head was subjected to first strand cDNA synthesis using oligo(dT)₂₀ reverse primer. To obtain full-length zAHCYL1 coding regions, gene-specific primers nested to the zAHCYL1 5'- and 3'-untranslated region were synthesized: MK350 (5'-CGACAGCTTGTTCTCCTTCC-3') and MK352 (5'-AAGAGCTCAGGCCAGACACA-3'), corresponding to exon 1 (nucleotides 58–77) and exon 2 (nucleotides 9–28), respectively, as the forward primers and MK351 (5'-AAGCCACAGACATCCTTTT-3'), corresponding to nucleotides 2288–2310, as the nested reverse primer. PCR products were cloned into pGEM-T Easy vector (Promega, Annandale, New South Wales, Australia) for sequencing.

Identification of Alternatively Spliced hAHCYL1—Alternative N-terminal splicing of hAHCYL1 was identified in humans using the dbEST data base available from NCBI. In order to identify sequences of authentic splice variants, we searched for ESTs that (i) contained sequence that overlapped substantially

with known hAH CYL1 cDNA and (ii) could be mapped to the chromosome band 1p12 for the hAH CYL1 gene (1).

Quantitative RT-PCR—Total RNA purified from zebrafish embryos at different stages of development (50–100 embryos/stage) using Trizol (Invitrogen) was treated with DNase I (Invitrogen) to remove contaminating genomic DNA and subjected to cDNA synthesis with random hexamers using Expand reverse transcriptase (Roche Applied Science). For quantitative RT-PCR analysis, the cDNA was combined with gene-specific forward and reverse primers for zAH CYL1A, zAH CYL1B, zAH CYL2, and zAH CY and a SYBR green master mix (QuantiTect SYBR PCR kit, Qiagen, Clifton Hill, Victoria, Australia) and subjected to real time PCR using a Rotorgene 3000 thermal cycler (Corbett Research, Mortlake, New South Wales, Australia). Zebrafish glyceraldehyde-3-phosphate dehydrogenase (GAPDH) was used for normalization of cDNA input. The primers were zAH CYL1A, MK279, and MK391 (5'-ACAGCGAGGTGAACATGAAC-3'); zAH CYL1B, MK279, and MK352; zAH CYL2, MK388 (5'-TCTTGGTGGGACGTTTGTG-3'), and MK390 (5'-ACCGAGCCCCATGAAGAT-3'); and zebrafish GAPDH, MK293 (5'-CCCAATGTCTCTGTTGTGGA-3'), and MK294 (5'-CGTGTAGAGCAATACCA-GCA-3'). The standard curves were generated using serially diluted gene-specific amplicons. The thermal cycling conditions were as follows: initial denaturation at 95 °C for 15 min, 45 cycles of 95 °C for 15 s, 58 °C for 15 s and 72 °C for 30 s, followed by melting temperature analysis (72–99 °C with 1 °C increments). Data analysis was performed using Rotorgene 5.0 software (Corbett Research). The amplification was specific as judged by melting temperature analysis, agarose gel analysis, and DNA sequencing of the amplicons. The experiments were performed in duplicate and repeated at least twice.

Production of Rabbit Anti-AH CYL1 Peptide Antibody—Rabbit polyclonal peptide antisera against the AH CYL1 C-terminal peptide were produced by immunizing New Zealand White rabbits with diphtheria toxoid-conjugated synthetic peptide CGPFPKNYYRY (Mimotopes, Clayton, Victoria, Australia) using a conventional schedule with Freund adjuvant at the Herston Medical Research Center (Herston, Queensland, Australia). The titer of the antibody against the peptide was assessed by enzyme-linked immunosorbent assay using an enzyme-linked immunosorbent assay plate (Maxisorb; Nalge Nunc, Rochester, NY) coated with streptavidin (Sigma) and biotinylated peptides for AH CYL1 (biotin-SGSGCGPFPKNYYRY). The antibody was purified with a series of affinity column chromatography using a HiTrap protein A and a HiTrap streptavidin (Amersham Biosciences) conjugated with the biotinylated C-terminal AH CYL1 peptide. The antibody reacted with both AH CYL1 and AH CY in Western blot analysis.

Zebrafish Maintenance and Collection of Embryos—Zebrafish were maintained under standard conditions as described (8) and used under the protocols approved by University of Queensland Animal Ethics Committee. Embryos were obtained from natural spawning of adult fish on a 14-h light/10-h dark cycle and were raised at 28 °C. Stages were determined by both hours postfertilization (hpf) and morphologic features (9). Photographs were taken on a SPOT digital camera setup (Diagnostic

Instruments Inc, Sterling Heights, MI) using a Leica S240 dissecting microscope equipped with an epifluorescent system.

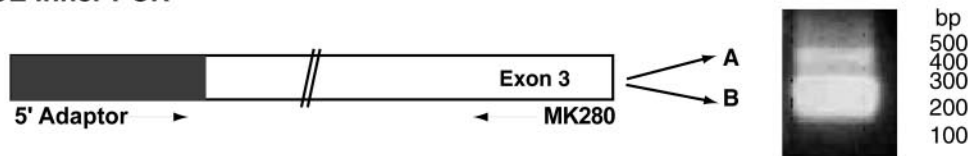
Morpholino Antisense Oligonucleotides against AH CYL1 for Microinjection—The morpholino antisense oligonucleotides MO1A (5'-TGGCATCCTCGCCACAGTCTGTCAT-3') and MO1B (5'-CATGGTTCATGTTCCCTGTGTGTGT-3') against zAH CYL1A and zAH CYL2 (see Fig. 1), and a standard control morpholino antisense oligonucleotide (5'-CCTCTTACCCTCAGTTACAATTTATA-3') were obtained from Gene Tools (Philomath, OR). Zebrafish embryos at the 1–2-cell stage were microinjected (0.5 nl/embryo) with the morpholino oligonucleotides (1, 0.5, or 0.2 mM) mixed with synthetic capped enhanced green fluorescent protein (EGFP), E1/EGFP, or E2/EGFP mRNA (0.125 mg/ml, described below).

Production of pCS2-hAH CYL1, pCS2-hAH CY, and pCS2-zAH CYL1 mRNA Synthesis Vectors—The cDNAs of human and zebrafish AH CYL1 and human AH CY cDNA, including 5'- and 3'-untranslated regions were cloned into the pCS2+ expression vector (10). Briefly, hAH CYL1A sequence was excised from the clone 211(1)B (1) using XbaI and SacI, and ligated into the corresponding sites available in pCS2+ to generate pCS2-hAH CYL1A. The human AH CY cDNA was amplified using RT-PCR from pooled human cDNA (from monocyte-derived dendritic cells and cell lines (*i.e.* L428 and HL60)) using primers MK276 (5'-CGGCCAGTTCCTGTTCC-3') and MK277 (5'-GCTCATGGTTCCTGTGG-3') using a *Taq* polymerase (Roche Applied Science). The PCR product was cloned into pGEM-T Easy vector for sequence confirmation. The insert was excised with NotI and SpeI, NotI site-blunted, and subcloned into pCS2+ with blunted BamHI and SpeI sites. The zAH CYL1A sequence was derived from the pGEM-T Easy vector clone (described above) and cloned into pCS2+ using a strategy similar to that described for the human AH CY clone. All plasmids were linearized with NotI for *in vitro* mRNA synthesis.

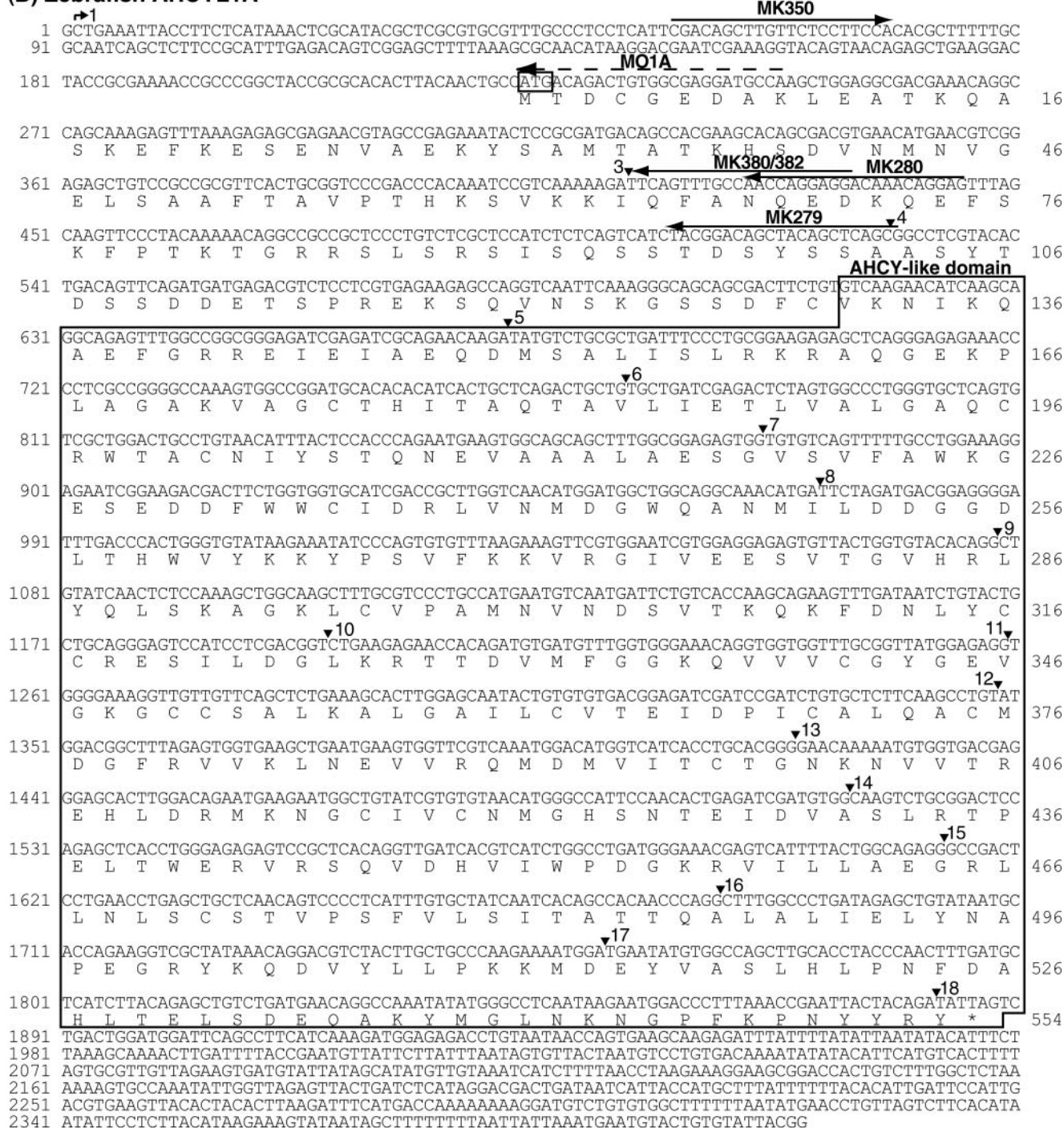
Production of pCS2-E1/EGFP and pCS2-E2/EGFP mRNA Synthesis Vectors—zAH CYL1 cDNAs encoded by the exon 1 and exon 2 were PCR-amplified with *Pfu* polymerase (Stratagene, La Jolla, CA) using sets of primers MK350/MK380 (5'-GCACCATGGCCTCCTGGTTGGCAAAGTAA-3', NcoI site underlined) for exon 1 and MK352/MK382 (5'-GCATCATGACCTCCTGGTTGGCAAAGTAA-3', RsaI site underlined) for exon 2, respectively (see Fig. 1). The PCR products were cloned into pCS2+EGFP digested with SmaI/NcoI or SmaI/RsaI so that the cloned exons were in frame with EGFP.

Capped mRNA Synthesis and Microinjection—Capped mRNA was synthesized using a SP6 mMessage mMachine kit (Ambion, Austin, TX). EGFP (an injection control) mRNA was prepared as described previously (10). RNA was purified by phenol/chloroform extraction followed by ethanol precipitation and resuspended to a concentration at 1.5 mg/ml, and integrity was checked by formaldehyde denaturing gel electrophoresis. Zebrafish embryos at the 1–2-cell stage were microinjected (0.5 nl/embryo) with the synthesized mRNA (1 mg/ml) mixed with EGFP mRNA (0.125 mg/ml). Only EGFP-positive embryos were examined at 12–28 hpf and scored according to the severity of their morphological

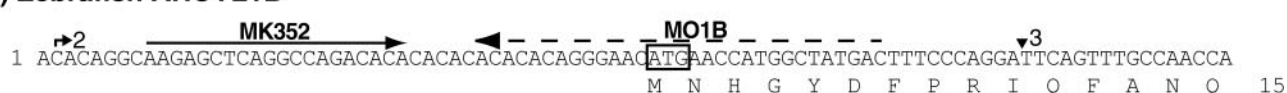
(A) 5'-RACE Inner PCR



(B) Zebrafish AHCYL1A



(C) Zebrafish AHCYL1B



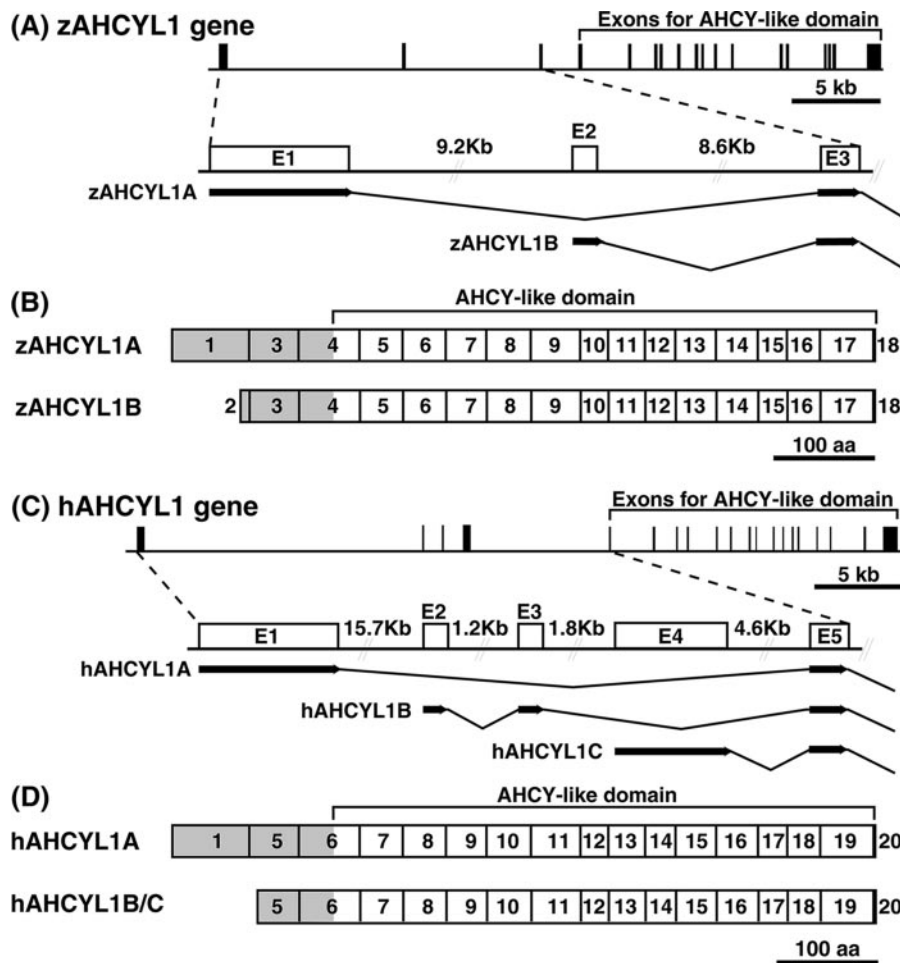


FIGURE 2. Genomic organization and alternative splicing of AHCYL1 in zebrafish (A and B) and humans (C and D). A, schematic representation of the zAHCYL1 gene and the alternative 5' exon splicing. The gene consists of 18 exons (E1–E18, indicated by boxes). B, deduced protein structure of zAHCYL1 variants. The two variants, zAHCYL1A and -B, differ at the N terminus of the protein due to the alternative use of either exon 1 or exon 2. The boxes indicate exons, and the numbers correspond to the exon number. The N-terminal hydrophilic domain is shaded gray. C, schematic representation of hAHCYL1 genome and the alternative exon usage to produce hAHCYL1 mRNA splicing variants (AHCYL1A–AHCYL1C). The gene consists of 20 exons (E1–E20, indicated by boxes). D, deduced protein structure of hAHCYL1 variants. Although the alternative splicing produces three variant mRNAs (AHCYL1A, B, and C), only two variant proteins are produced, because both exon 2/3 and exon 4 encode only 5'-untranslated sequence, and the translation start site appears to be within the common exon 5. aa, amino acids.

defects. Embryos injected with EGFP mRNA at 1.2 mg/ml were used as injection controls.

Depletion of Intracellular Calcium Stores—Thapsigargin treatment of embryos was performed according to Westfall *et al.* (11). Briefly, a 5 mM thapsigargin (Sigma) stock solution was made in Me₂SO. 32–64-cell stage embryos were incubated with 5 μ M thapsigargin diluted in egg medium (8). Me₂SO-only incubations were used as a negative control. After a 1-h incubation, embryos were washed extensively in egg medium and incubated at 28 °C in embryo media until required.

and incubated sequentially with the rabbit anti-AHCYL1 peptide antibody (5 μ g/ml) and horseradish peroxidase-conjugated goat anti-rabbit IgG (1:5000 dilution; Chemicon, Boronia, Victoria, Australia) and the signals detected with enhanced chemiluminescence (Pierce).

RESULTS

Cloning of zAHCYL1 and Its Genomic Organization—The AHCYL1 gene is highly conserved among species (e.g. 100% protein

Western Blot Analysis—Zebrafish embryos (1–2-cell stage) were injected with synthetic hAHCYL1, zAHCYL1, or hAHCYL1 mRNA (1.5 mg/ml) in combination with EGFP mRNA and incubated for 6 h. EGFP-positive embryos were harvested and lysed with 1% Triton X-100, 50 mM Tris-HCl, pH 7.4, and a protease inhibitor mixture (Complete; Roche Applied Science), 1 mM phenylmethylsulfonyl fluoride (Sigma), and 5 mM EDTA, and the lysate was cleared by centrifugation at 20,000 \times g for 10 min at 4 °C. The protein concentration was determined by a BCA protein assay (Pierce) using bovine serum albumin as standard. The lysate was aliquoted and stored at –70 °C until use. For positive controls, COS-7 cells in two 100-mm dishes were transfected with pCS2-hAHCYL1 or pCS2-hAHCYL1 (5 μ g/dish) using Eugene 6 (Roche Applied Science) according to the manufacturer's protocol and incubated for 48 h. The cells were lysed with the lysis buffer, and protein concentration was determined as above.

The lysate from the zebrafish embryos (250 μ g) and COS-7 cell transfectants (20 μ g) was fractionated with a 4–12% gradient SDS-polyacrylamide gel (NuPAGE; Invitrogen) in reducing conditions and transferred onto a polyvinylidene difluoride membrane (PVDF-Plus, Osmonics, Westborough, MA). The membrane was blocked with 5% nonfat skim milk, 0.1% Tween 20 (Sigma) in phosphate-buffered saline

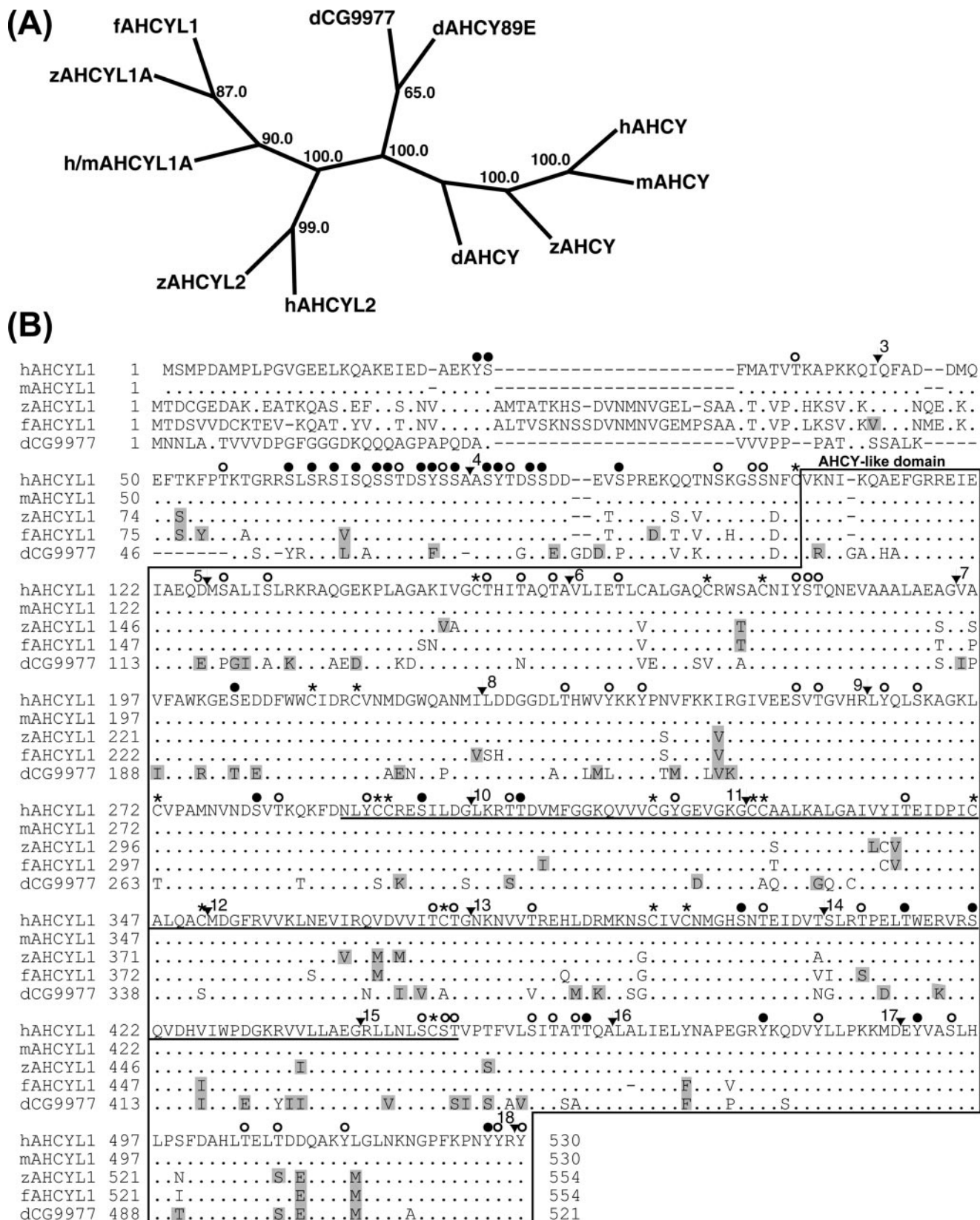
FIGURE 1. Molecular cloning of zAHCYL1 cDNAs. A, 5'-RACE cloning of alternatively spliced zAHCYL1 variant cDNAs. The cloning strategy is depicted in the left panel. Zebrafish total RNA was subjected to 5'-RACE, and the product was resolved in a 2% agarose gel and visualized with ethidium bromide (right panel). DNA standards are indicated on the right. B, the complete cDNA and amino acid sequence of zAHCYL1A encoded by 17 exons, including exon 1 and exons 3–18. C, the partial cDNA and amino acid sequence of zAHCYL1B encoded by exon 2 and the beginning of exon 3. The solid arrows indicate the position of gene-specific primers used for 5'-RACE and the production of pCS2-E1/EGFP and pCS2-E2/EGFP. The dashed arrows indicate the target sites for the morpholino antisense oligonucleotides (MO1A and MO1B) against zAHCYL1A and -B, respectively. Exon/intron junctions are indicated by vertical arrows and numbered according to exon number. The kinked arrows indicate start sites identified by 5'-RACE.

Role of AHCYL1 on Zebrafish Development

identity between human and mouse) (1). To clone the zAHCYL1, we conducted a BLAST search using the coding sequence for hAHCYL1 cDNA (GenBank™ accession number AF315687) to search the NCBI zebrafish EST data base. The ESTs obtained were

aligned to establish a consensus zAHCYL1 cDNA sequence, which was confirmed by RT-PCR and DNA sequencing.

To determine the transcriptional start site on zAHCYL1 mRNA, we performed 5'-RACE analysis using primers



nested in the 5'-zAH CYL1 cDNA in the adult zebrafish head-derived cDNA library. This resulted in two PCR products (~450 and 250 bp) (Fig. 1A). Sequencing analysis revealed that these two products corresponded to two zAH CYL1 mRNA variants with mutually exclusive transcription start sites termed zAH CYL1A and zAH CYL1B (Fig. 1, B and C). The zAH CYL1A sequence corresponded to the zAH CYL1 sequence obtained by EST data base search and confirmed using RT-PCR (Fig. 1B). This was identified as the ortholog of hAH CYL1 (described below). The zAH CYL1B sequence contained a previously uncharacterized 46-bp alternative 5'-untranslated region plus an alternative coding sequence for the N-terminal 9 amino acids, assuming that the first ATG in the sequence is the initiation codon (Fig. 1C). These results suggested that at least two alternatively spliced variants of zAH CYL1 were present.

To determine the full genomic structure of zAH CYL1A and -B, we performed a BLAST search of the Ensembl zebrafish genomic sequence data base. One BAC clone (GenBankTM accession number AL773601) contained all of the cDNA sequences, and we determined the intron-exon boundaries using the "GT-AG" splice site consensus by comparing the genomic sequence with these cDNA sequences. We found the zAH CYL1 gene consisted of 18 exons spanning 39 kb (Fig. 2A). The zAH CYL1A transcript was encoded by 17 exons (with exon 2 spliced out), and the last 15 exons encoded the AH CY-like domain, similar to hAH CYL1. The zAH CYL1B transcript is also encoded by 17 exons but uses exon 2, located 9.2 kb downstream of exon 1, as an alternative first exon.

The putative zAH CYL1A protein (encoded by exons 1 and 3–18) consists of 554 amino acids with an N-terminal hydrophilic domain (130 amino acids; exons 1, 3, and 4) and an AH CY-like domain (424 amino acids; exons 4–18) (Fig. 2B). The putative initiation codon was identified by comparing the zAH CYL1 protein to that of *T. rubripes* AH CYL1 protein (assigned GenBankTM accession number BK005364). The zAH CYL1B protein (exons 2 and 3–18) consists of 500 amino acids with the N-terminal hydrophilic domain being only 76 amino acids (exons 2–4) (Fig. 2B). Its initiation codon was identified as the first methionine in exon 2.

Next we investigated possible alternative usage of 5' exons in hAH CYL1 (now termed hAH CYL1A). By carrying out an extensive analysis of human EST sequences, we identified two ESTs encoding previously uncharacterized, alternatively spliced hAH CYL1 mRNAs termed hAH CYL1B and -C (Fig. 2C). hAH CYL1B was represented by two ESTs (GenBankTM accession numbers T19009 and BI460083) encoded by two separate exons (*i.e.* exons 2 and 3) joined to exon 5 (Fig. 2C). hAH CYL1C was represented by three ESTs (GenBankTM

accession numbers AU279527, AL036027, and BF930049), which contained another alternative exon 4 (Fig. 2C). These three newly identified exon sequences (exons 2–4) could be joined by proper intron/exon junctions to exon 5. However, the only putative initiation codon appeared in exon 5, suggesting that these exons encoded alternative 5'-untranslated regions for truncated hAH CYL1 proteins, which lacked nearly half of the N-terminal hydrophilic domain (Fig. 2D).

AH CYL1 Protein Is Evolutionarily Conserved among Species—We used phylogenetic analysis to assess the evolutionary relationships between the orthologs of AH CYL1, AH CY, and the other member of the AH CY-like protein family in zebrafish, zAH CYL2 (GenBankTM accession number AAH5951), a possible ortholog of hAH CYL2 (GenBankTM accession number BC024325) (3). The AH CYL1 genes were distinguished from AH CY genes, suggesting that AH CYL1 diverged early from AH CY and evolved separately (Fig. 3A). Furthermore, both zebrafish and human AH CYL2 were more closely related to AH CYL1 than AH CY. Fruit fly AH CY-like proteins (CG9977 and AH CY89E), which also have an N-terminal hydrophilic domain and an AH CY-like domain, clustered with AH CYL1 and AH CYL2.

The amino acid comparison between the human and zebrafish AH CYL1A proteins show 93% identity and 97% similarity, across the region encoded by human exons 5–20 and the zebrafish exons 3–18 (Fig. 3B). Comparison with additional AH CYL1A orthologs (from mouse, fugu fish, and fruit fly) confirmed that the AH CY-like domains, including the NAD⁺ binding domains (161 amino acids) were highly conserved in the AH CYL1 orthologs (Fig. 3B). In addition to highly conserved Cys, 27 predicted Ser/Thr/Tyr phosphorylation sites were conserved among all vertebrates analyzed, 16 of which were clustered in the N-terminal hydrophilic domain (Fig. 3B). The majority of these Ser/Thr/Tyr residues were also conserved in the fruit fly AH CYL protein. The protein sequences encoded by exon 1 are highly diverse between species, with zAH CYL1 proteins being 24 amino acids longer than hAH CYL1 at the N terminus. These data suggest that Ser/Thr/Tyr phosphorylation and NAD⁺ binding are likely to play an important role in AH CYL1 function.

zAH CYL1A and -B and zAH CYL2 mRNA Are Regulated during Embryogenesis—We investigated the expression of zAH CYL1A and -B, zAH CYL2 and zAH CY mRNA in developing zebrafish embryos by real time RT-PCR (Fig. 4). Zebrafish GAPDH was used to normalize the cDNA input. zAH CYL1A was first apparent at the shield stage of embryos, and its expression was steadily increased until the 25-somite stage. At 25 hpf, its expression decreased markedly to half that of the 25-somite stage. zAH CYL1B mRNA expression

FIGURE 3. The AH CYL1 genes are evolutionarily conserved among species. A, phylogenetic analysis of AH CYL homologs. Protein sequences from AH CY/L AH CY-like domains of AH CY, AH CYL1, and AH CYL2 orthologs were subjected to phylogenetic analysis with 100 bootstrapping cycles. The numbers indicate the bootstrap values generated using the neighbor joining method. *Drosophila* AH CY (dAH CY) was chosen as the outgroup. The tree is unrooted. Homologs included are as follows: human and mouse AH CYL1A (identical protein sequences), zAH CYL1A, fugu fish AH CYL1 (fAH CYL1), hAH CYL2, zAH CYL2, fruit fly AH CY-like proteins (dCG9977 and dAH CY89E), hAH CY, mouse AH CY (mAH CY), and zebrafish AH CY (zAH CY). B, amino acid comparison between five AH CYL1A orthologs from human, mouse, zebrafish, fugu fish, and fruit fly (dCG9977). AH CY-like domains are boxed. Amino acids identical to hAH CYL1 are indicated by dots. Conservatively replaced amino acids are shaded by gray boxes. Gaps are shown as dashes. The NAD⁺ binding motif is underlined. The circles and asterisks indicate conserved Ser/Thr/Tyr and Cys in vertebrate AH CYL1A orthologs, respectively. The filled circles indicate potential Ser/Thr/Tyr phosphorylation sites. The vertical arrows indicate the exon-intron junctions of zAH CYL1A (see Fig. 1).

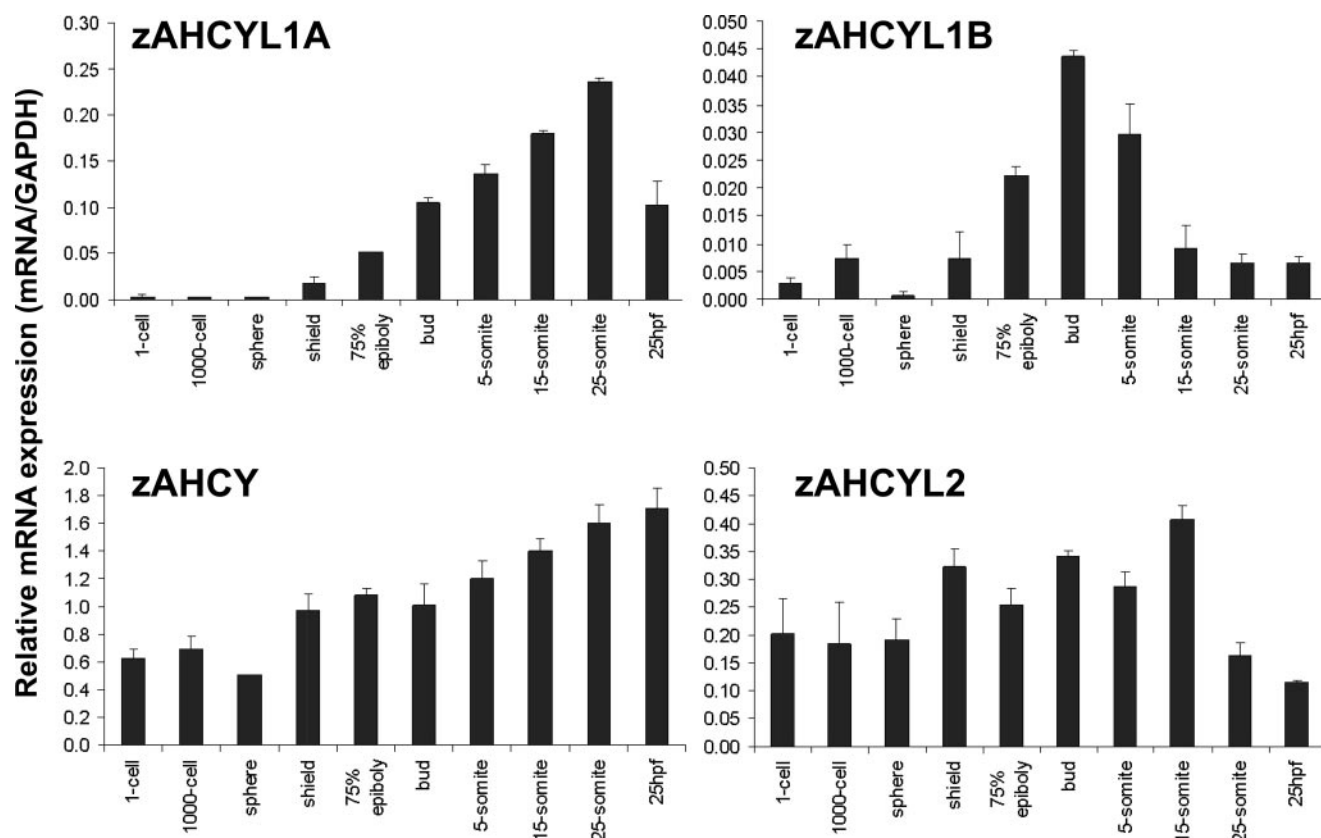


FIGURE 4. The expression of zAHCYL1A and -B and zAHCYL2 mRNA is regulated during embryogenesis. Total RNA purified from various developmental stages of zebrafish embryos were subjected to real time RT-PCR analysis for quantitation of zAHCYL1A, zAHCYL1B, zAHCYL2, and zAHCY mRNA. Zebrafish GAPDH was used to normalize the cDNA input.

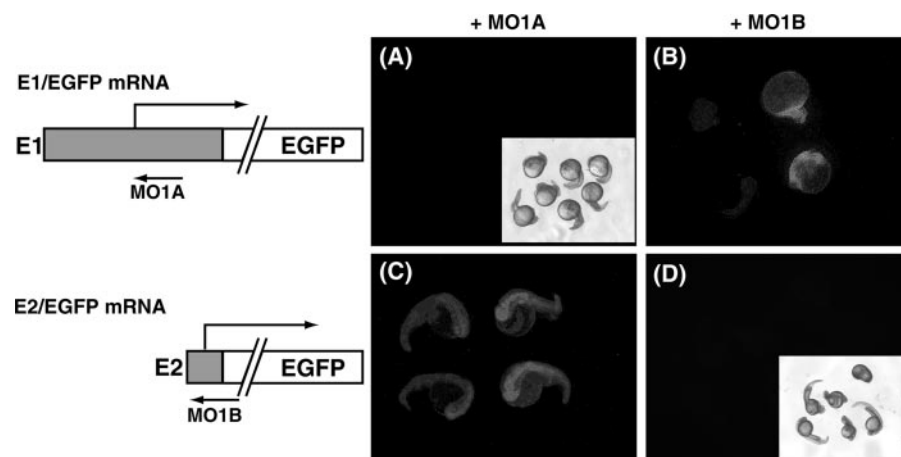


FIGURE 5. The morpholino oligonucleotides (MO1A and MO1B) against zAHCYL1A and -B specifically reduce the target gene expression. The fusion mRNA encoding EGFP and the zAHCYL1 exon 1 (E1, containing the MO1A target) (A and B) or the exon 2 (E2, containing the MO1B target) (C and D) was coinjected with the MO1A or MO1B, and expression of EGFP was analyzed by epifluorescence microscopy. The insets show the same field viewed by light microscopy.

increased from very low levels at the shield stage, peaking at the bud stage. Its expression then decreased to very low levels by the 15-somite stage and remained low until 25 hpf. zAHCYL1B mRNA expression levels were much lower overall than those of zAHCYL1A (<20%). In contrast to the regulation of zAHCYL1A and -B mRNA during development, zAHCY mRNA was present before cell division and expressed at much higher levels in developing embryos. Its

increase throughout development was consistent with the proposed role of zAHCY as a housekeeping gene. Finally, zAHCYL2 mRNA was also present before cell division at high levels and remained so until the 15-somite stage before decreasing markedly at the 25 hpf stage to levels similar to zAHCYL1A. These data indicated that zAHCYL1A and -1B expression underwent significant regulation and that both were likely to be important in zebrafish embryogenesis.

Suppression of zAHCYL1A and -B by the Morpholino Antisense Oligonucleotides Induces Ventralized Morphologies in Zebrafish Embryos—To investigate the function of zAHCYL1A and B in developing

embryos, we used morpholino antisense oligonucleotides against zAHCYL1A and -B. First, we examined the specificities of the morpholino oligonucleotides by coinjecting the synthetic fusion mRNAs containing zAHCYL1 exon 1 (E1/EGFP mRNA, zAHCYL1A-specific) or exon 2 (E2/EGFP mRNA, zAHCYL1B-specific) fused in frame with EGFP and the gene-specific morpholinos (MO1A and MO1B for zAHCYL1A and -B, respectively) into 1–2-cell stage

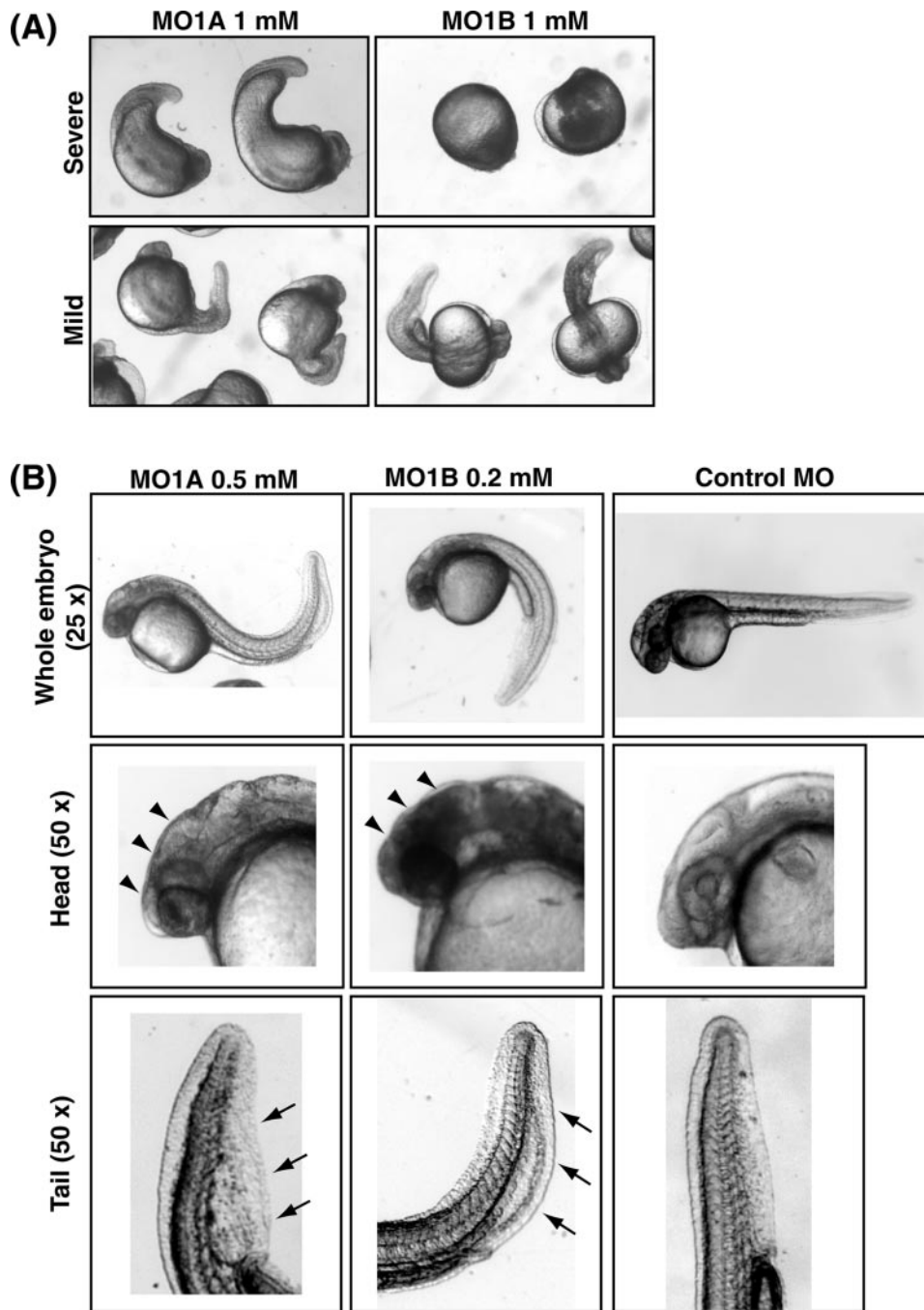


FIGURE 6. zAHCYL1 gene knockdown by MO1A or MO1B injection induces ventralization in zebrafish embryos. A, zebrafish embryos were injected with 1 mM MO1A or -1B and observed at 24 hpf. B, zebrafish embryos were injected with 0.5 mM MO1A or 0.2 mM MO1B and observed at 24 hpf. The standard control MO did not induce any gross phenotypes. The arrowheads and arrows indicate necrotic heads and expanded ventral tail fins, respectively. Magnification for whole embryos is $\times 25$; magnification for partial embryos is $\times 50$.

zebrafish embryos. The embryos were incubated overnight, and the gene-specific morpholino effects were assessed by the EGFP expression levels in the embryos. As shown in Fig. 5, MO1A suppressed the translation of the E1/EGFP mRNA completely, but not that of the E2/EGFP mRNA. Conversely, MO1B abolished E2/EGFP mRNA translation, but not that of E1/EGFP mRNA translation, indicating that MO1A and MO1B could inhibit specifically zAHCYL1A and -B translation, respectively.

When MO1A at 1 mM were injected into 1–2-cell stage zebrafish embryos and incubated overnight, the resultant embryos were often necrotic, and the surviving embryos showed severe and gross body axis deformities (Fig. 6A, Table 1). Injection of the MO1A at 0.5 mM produced a ventralized morphology, with abnormally developed and necrotic brain structures and expanded ventral tail fin tissue (Fig. 6B). Injection of further diluted MO1A had no morphological effect (data not shown). Injection of 1 mM or 0.5 mM MO1B resulted in similar numbers of severely deformed embryos (Fig. 6A). Injection of MO1B diluted further to 0.2 mM produced a ventralized morphology similar to that observed with the 0.5 mM MO1A injections (Fig. 6B). The apparent potency of MO1B compared with MO1A may be because zAHCYL1B mRNA was less abundant (see Fig. 4). Embryos injected with a control morpholino at 1 mM showed no abnormal morphologies. The similar morphologies, which were observed after the MO1A and MO1B injections, suggested that zAHCYL1A and -B have similar functions.

Microinjected Synthetic hAHCYL1A and hAHCYL1B mRNA Are Translated into Cognate Proteins in Zebrafish Embryos—The zAHCYL1 antisense morpholino studies showed that AHCYL1 might play a role in dorsalization, and the mRNA expression data suggested that its function was different from that of AHCYL1 (see Fig. 4). Therefore, we hypothesized that AHCYL1 overexpression in zebrafish embryos would induce dorsalized phenotypes and that this outcome would differ from that resulting from AHCYL1 overexpression. To test this, we first investi-

gated the translation of the injected synthetic mRNAs into the cognate proteins. The capped mRNA encoding hAHCYL1A and hAHCYL1B, synthesized using pCS2-hAHCYL1A and pCS2-hAHCYL1B as templates, were injected into 1–2-cell stage zebrafish embryos. The embryos were incubated for 6 h, lysed in a lysis buffer, and subjected to Western blot analysis using the anti-hAHCYL1 peptide antibody, which binds to both AHCYL1 and hAHCYL1. As shown in Fig. 7, the embryos injected with the hAHCYL1A mRNA expressed a substantial 58.7-kDa

TABLE 1

Summary of zebrafish morphologies after mRNA injection of morpholino oligonucleotides against zAHCYL1A and -B

Zebrafish embryos (at the 1–2-cell stage) were microinjected with morpholino oligonucleotides (MO) as indicated. Embryos were observed at 24 hpf for morphological defects.

Treatment	<i>n</i>	Necrotized	Abnormal	Normal
1 mM MO1A	110	5 (4.5%)	102 (92.7%)	3 (2.7%)
0.5 mM MO1A	30	0 (0%)	24 (80%)	6 (20%)
0.2 mM MO1A	49	0 (0%)	2 (4.1%)	47 (95.9%)
1 mM MO1B	70	56 (80%)	11 (15.7%)	3 (4.3%)
0.2 mM MO1B	52	11 (21.2%)	41 (78.8%)	0 (0%)
Standard control MO	73	0 (0%)	4 (4.5%)	69 (94.5%)
Uninjected	111	0 (0%)	2 (1.8%)	109 (98.2%)

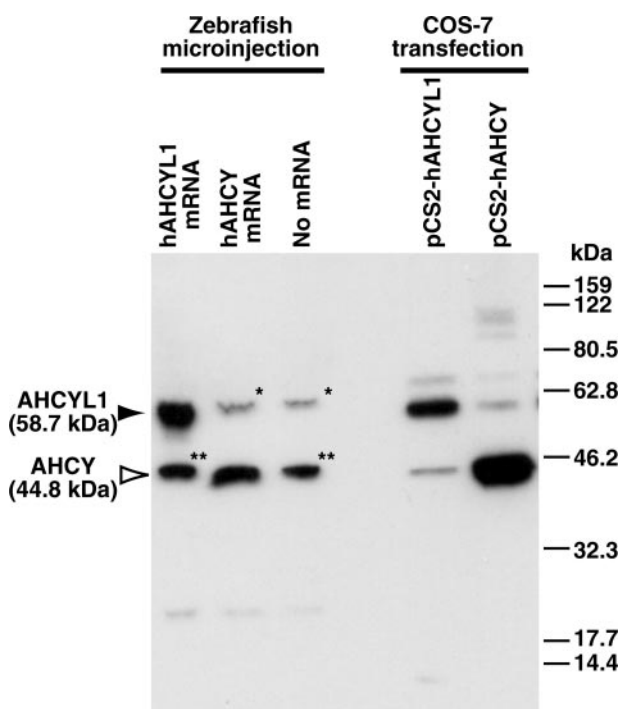


FIGURE 7. Translation of injected synthetic mRNA in zebrafish embryos. Zebrafish embryos (1–2-cell stage) were injected with synthetic hAHCYL1 and hAHCY mRNA and incubated for 6 h. The embryos were lysed and subjected to Western blot analysis for the cognate proteins. Cell lysate from COS-7 cells transfected with hAHCYL1 or hAHCY expression vector was used as positive control. The *single* and *double* asterisks indicate the position of endogenous zAHCYL1 and zAHCY, respectively. Molecular mass standards are indicated on the right.

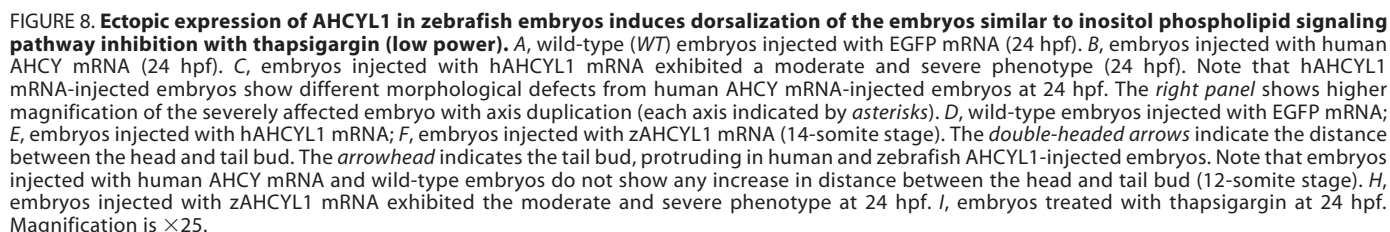
protein band corresponding to the hAHCYL1 protein, compared with the embryos injected with the hAHCY mRNA or to uninjected control embryos. The hAHCYL1 protein translated in zebrafish embryos was the same size as the AHCYL1 protein expressed in the COS-7 cells transiently transfected with the pCS2-hAHCYL1. The hAHCY mRNA was also translated into the protein in the zebrafish embryos as well; however, the expression levels did not change markedly because of high levels of endogenous zAHCY.

Microinjection of AHCYL1A mRNA Induces Dorsalized Morphologies in Zebrafish Embryos—The high levels of conservation of AHCYL1A proteins between species suggested that these proteins may have similar cross-species function. We injected the synthetic hAHCYL1A mRNA and hAHCY into the 1–2-cell stage zebrafish embryos and examined them after overnight incubation (Figs. 8 and 9). Those embryos injected

with hAHCYL1A mRNA displayed marked morphological defects, which were categorized based on the severity according to Mullins *et al.* (12) (Table 2). During the segmentation stage, the moderately affected embryos (C1–C3 grade) were characterized by a shortened protruding tail bud. The tail bud did not extend around the yolk as in wild type but rather protruded from the yolk sac and was slightly enlarged (Fig. 8E). The heads of these embryos were also slightly enlarged, often exhibiting a prominent square shape. These embryos also exhibited an increase in the distance between the head and tail bud, suggesting inhibition of convergent extension movement (Fig. 8E). At the pharyngula stage, the majority of hAHCYL1A mRNA-injected embryos displayed prominent tail shortening/kinking defects (Fig. 8C). Severely affected embryos (C4–C5 grade) had more pronounced changes characterized by a complete loss of posterior structure and severely reduced anterior structure (Fig. 8C; see below) with a duplicated axis also evident in some embryos (Fig. 8C, *higher magnification*). These hAHCYL1 mRNA-induced morphological defects were consistent with the features associated with dorsalization (12). Only 1% of embryos injected with EGFP mRNA showed abnormalities, indicating that the morphological defects in hAHCYL1 mRNA-injected embryos were specific to hAHCYL1A overexpression. In contrast, the majority of hAHCY mRNA-injected embryos displayed normal convergent extension movement comparable with the wild type at segmentation stage, indicating that gastrulation movements during segmentation were not disrupted (Fig. 8, B and G). These data suggested that AHCYL1A differed from AHCY in function.

It was possible that differences in protein structure (mostly localized at the N-terminal hydrophilic domain) between human and zebrafish AHCYL1A mediated species-specific function of AHCYL1A. Thus, we examined the effect of zAHCYL1A overexpression during embryogenesis (Fig. 8 and Table 2). Embryos injected with zAHCYL1A mRNA displayed morphological defects similar to those with hAHCYL1 expression. At the segmentation period, the moderately affected embryos (C1–C3) displayed a protruding tail bud similar to that seen in hAHCYL1 mRNA-injected embryos (Fig. 8F). Unlike hAHCYL1A mRNA injected embryos, the head shape appeared to be normal in zAHCYL1 mRNA-injected embryos. Interestingly, the transient Kupffer's vesicle appears enlarged in zAHCYL1A mRNA-injected embryos. At the pharyngula stage, embryos displayed a shortened and kinked tail structure similar to that observed with hAHCYL1 mRNA-injected embryos (Fig. 8H). Those embryos with a moderate dorsalized morphologies (C1–C3) showed reduced circulation (data not shown), thickened/split notochord, and loss of ventral tail tissue (Fig. 9). More severely affected embryos exhibited severe dorsalization (C4–C5 grade) characterized by complete loss of posterior structure as seen in hAHCYL1A mRNA-injected embryos (Fig. 8H), suggesting that function of AHCYL1A orthologs was largely conserved among species.

Dorsalized morphologies of zebrafish embryos were evident when the phosphatidylinositol cycle was inhibited (11). The phosphatidylinositol cycle is responsible for generating IP₃R-dependent intracellular Ca²⁺ release through the action of a second messenger, IP₃ (13). Because AHCYL1 binds to the IP₃R



involved in phosphatidylinositol/ Ca^{2+} signaling, inducing dorsalized phenotypes in zebrafish embryos.

AHCYL1 was presumed to be a protein with AHCY-like enzymatic activity because of its high protein identity with AHCY. We now provide evidence that AHCYL1 differs from AHCY both in its evolution and function.

JOURNAL OF BIOLOGICAL CHEMISTRY 22481

Role of AHCYL1 on Zebrafish Development

during *X. laevis* embryogenesis (17). Moreover, it complexes with mRNA(guanine-7-)methyltransferase and RNA polymerase II (18), further suggesting that AHCY contributes to fundamental cellular functions as well as embryonic development.

Protein sequences for AHCY orthologs have been identified from more than 30 different species, including bacteria, plants, and vertebrates (2). Our analysis of various prokaryotic and eukaryotic genomes revealed that the AHCY-like protein family members (AHCYL1 and AHCYL2) (1, 3) are only present in segmented multicellular organisms (*i.e.* vertebrates and insects but not nematode, yeast, malaria, and prokaryotes), whereas AHCY orthologs are present in all organisms examined (Table 3). Taken together with the phylogenetic analysis (Fig. 3), we concluded that AHCYL1 and AHCYL2 form an evolutionarily distinct family of molecules, which are likely to have evolved a novel function required in higher organisms. This fits with the finding that AHCYL1 lacks important residues found in AHCY that are necessary for AHCY enzymatic function (1).

Recently, an IP₃R-binding protein isolated from a rat brain extract using an IP₃R fusion protein affinity column was identified as AHCYL1 (6). AHCYL1 binding to IP₃R was mediated

by the N-terminal hydrophilic domain and abolished by alkali phosphatase treatment, suggesting that phosphorylation of AHCYL1 is essential for the binding. Because many putative Ser/Thr/Tyr phosphorylation sites in AHCYL1 N-terminal hydrophilic domain are conserved among species (Fig. 3), it is likely that the phosphorylation of this domain is important for AHCYL1 binding to IP₃R. Although the functional consequence of AHCYL1 binding to IP₃R has yet to be determined, it may modulate Ca²⁺ release by IP₃R. The hydrolysis of phosphatidylinositol 4,5-bisphosphate in response to cell surface receptor activation results in the production of IP₃, which in turn binds to IP₃R to release Ca²⁺ stored in the endoplasmic reticulum. The resulting Ca²⁺ release regulates the activation of numerous downstream targets important for many cellular and developmental processes in all higher organisms, including fruit fly, zebrafish, and mouse (13, 19–21). For example, the increase of AHCYL1 mRNA that we observed in human DC is entirely consistent with Ca²⁺ signaling-mediated control of DC function (22–25).

Kume *et al.* (26) produced a series of monoclonal antibodies against *Xenopus* IP₃R and showed that injection of these monoclonal antibodies into the ventral blastomeres of 4-cell stage *Xenopus* embryos converted ventral mesoderm to dorsal mesoderm, resulting in dorsalization of the embryos. Interestingly, no dorsalization was observed when these monoclonal antibodies were injected dorsally (26). Westfall *et al.* (11) further showed that injection of one of these monoclonal antibodies (clone 1G9) into zebrafish embryos induced dorsalization. Furthermore, depletion of intracellular Ca²⁺ by thapsigargin induced dorsalized zebrafish embryos (11). These results strongly suggest that the Ca²⁺ signaling mediated by IP₃R is important for the normal development of ventral but not dorsal structures in developing embryos, and perturbation of ventral IP₃R function induces dorsalization of embryos. We showed that morpholino suppression of zAHCYL1 induced ventralization of zebrafish embryos, and conversely AHCYL1 overexpression by mRNA injection

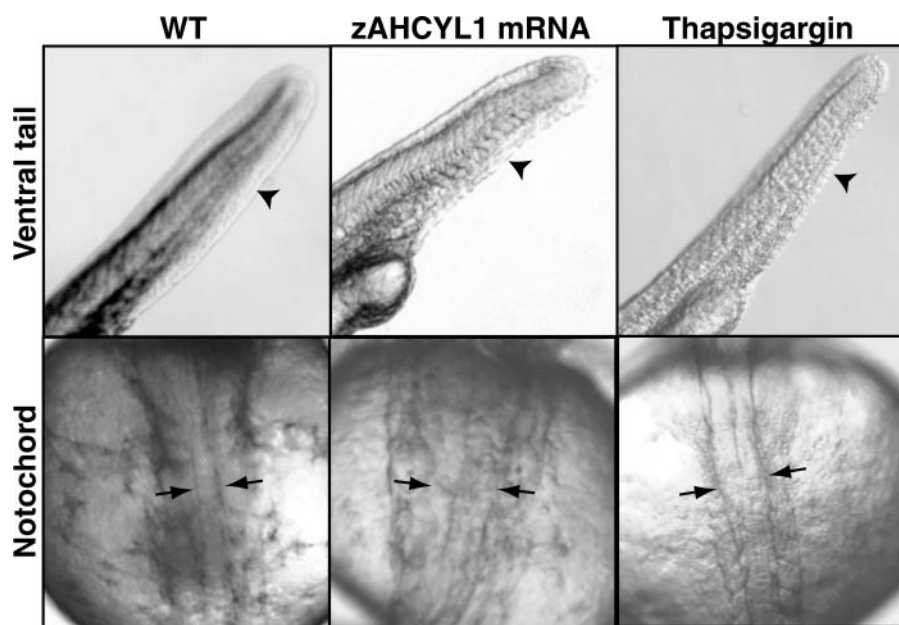


FIGURE 9. Dorsalization of zebrafish embryos by zAHCYL1 mRNA injection is similar to inositol phospholipid signaling pathway inhibition with thapsigargin (magnification $\times 50$). Ventral tails (*upper panels*) and notochords (*lower panels*) of wild-type (WT) embryos (*left panels*), zAHCYL1 mRNA-injected embryos (*center panels*), and thapsigargin-treated embryos (*right panels*) are shown. Note that both AHCYL1 mRNA-injected and thapsigargin-treated embryos show the loss of ventral tail tissue (*single arrowheads in upper panels*) and thickened/split notochord (*double arrowheads in lower panels*) when compared with wild-type embryos.

TABLE 2

Summary of zebrafish morphologies after mRNA injection or thapsigargin treatment

Zebrafish embryos were microinjected with synthesized mRNA at the 1–2-cell stage or treated with thapsigargin at the 32–64-cell stage. Embryos were observed at 24 hpf for morphological defects and characterized according to the dorsalization phenotypes C1–C5 (12).

Treatment	<i>n</i>	C1–C3	C4–C5	Other ^a	Normal
hAHCYL1A (1000 μ g/ml)	97	42 (43.3%)	12 (12.4%)		43 (44.3%)
zAHCYL1A (1000 μ g/ml)	84	50 (59.5%)	8 (9.5%)		26 (31.0%)
hAHCY (1000 μ g/ml)	89	4 (4.5%)	0 (0%)	12 (13.5%)	73 (82.0%)
GFP (1200 μ g/ml)	130	1 (0.7%)	0 (0%)	7 (5.4%)	122 (93.8%)
Thapsigargin (5 μ M)	155	5 (3.2%)	118 (76.1%)	32 (20.6%)	0 (0%)

^a Morphologies not seen in AHCYL1 microinjections.

TABLE 3

Distribution of AHCY and AHCYL genes in various organisms

Publicly available genome/EST databases were scanned for the presence of orthologs.

	AHCY	AHCYL
Prokaryotic species		
<i>Agrobacterium tumefaciens</i> (rhizobiaceae)	+	—
<i>Caulobacter crescentus</i> (caulobacter)	+	—
<i>Chlorobium tepidum</i> (green sulfur bacteria)	+	—
<i>Clostridium thermocellum</i> (clostridium)	+	—
<i>Leptospira interrogans</i> (spirochaetales)	+	—
<i>Pseudomonas aeruginosa</i> (pseudomonas)	+	—
<i>Streptomyces coelicolor</i> (actinobacteria)	+	—
<i>Xanthomonas axonopodis</i> (other gamma)	+	—
Eukaryotic species		
<i>S. cerevisiae</i> (yeast)	+	—
<i>P. falciparum</i> (malaria)	+	—
<i>C. elegans</i> (nematode)	+	—
<i>A. gambiae</i> (mosquito)	+	+
<i>D. melanogaster</i> (fruit fly)	+	+
<i>T. rubripes</i> (fugu fish)	+	+
<i>D. rerio</i> (zebrafish)	+	+
<i>X. laevis</i> (frog)	+	+
<i>G. gallus</i> (chicken)	+	+
<i>Mus musculus</i> (mouse)	+	+
<i>Homo sapiens</i> (human)	+	+

induced dorsalization of zebrafish embryos (Figs. 6–9). These results are consistent with the notion that AHCYL1 binding down-regulates the function of IP₃R by its competition with IP₃ for IP₃R binding (6). Moreover, AHCYL1 overexpression inhibits IP₃R-mediated Ca²⁺ release, causing dorsalization, and AHCYL1 suppression overactivates IP₃R-mediated Ca²⁺ release, causing ventralization. Our data, although indirect, suggest that AHCYL1 behaves as a regulator to control IP₃R activation levels and thus has major impacts on embryogenesis.

We isolated two alternative splice forms of zAHCYL1 differing only in their N-terminal sequences. Similar alternative splicing was documented for hAHCYL1 (Fig. 2). The N-terminal hydrophilic domain of AHCYL1 is essential for binding to the IP₃R (6), therefore it is possible that the differences in the N-terminal of the protein encoded by alternative 5' exons may alter the binding affinity or specificity of the AHCYL1 molecule to different IP₃R isoforms. There are three known isoforms of IP₃R, which differ in their tissue distribution, IP₃ sensitivity, and Ca²⁺ dependence (27). The second AHCY-like molecule, AHCYL2, has a very similar AHCY-like domain but quite a distinct N-terminal hydrophilic domain (1, 3). There is no information on AHCYL2 function or its IP₃R binding ability, but its high structural similarity to AHCYL1 suggests that it has a similar function. They may represent even further potential for differential and competitive regulatory binding capacity to the IP₃R isoforms, entirely consistent with the complexity of regulation of the crucial Ca²⁺ signaling pathway.

The mechanism of AHCYL1-binding to IP₃R and the subsequent IP₃R regulation of Ca²⁺ signaling is likely to be complex: (i) the binding of AHCYL1 to IP₃R requires phosphorylation of AHCYL1, probably mediated by protein kinases downstream of intracellular calcium release (e.g. protein kinase C, Ca²⁺/calmodulin-dependent protein kinases, and/or the other protein kinases concomitantly activated with the inositol phospholipid signaling pathway), (ii) there is in excess of nonphosphorylated free AHCYL1 within the cytoplasm, (iii) protein phosphatases are also

likely to play a role in maintaining the equilibrium between non-phosphorylated and phosphorylated AHCYL1, and (iv) these phosphatases must also be regulated within the inositol phospholipid signaling cascades. There are no AHCYL1-negative cell lines readily available for experimentation.⁴ This plus these complex interactions make it difficult to obtain direct evidence for AHCYL1 function. We are currently performing experiments that will address AHCYL1 function more directly, using cells from AHCYL1 gene-deleted mice.

Acknowledgments—We thank Ronald P. Gladue for advice. We also acknowledge Seema Khan and Kylie McDonald for technical assistance.

Note Added in Proof—Devogelaere *et al.* (28) showed recently that AHCYL1 binds directly to IP₃R and inhibits IP₃ binding and IP₃-induced Ca²⁺ release.

REFERENCES

- Dekker, J. W., Budhia, S., Angel, N. Z., Cooper, B. J., Clark, G. J., Hart, D. N., and Kato, M. (2002) *Immunogenetics* **53**, 993–1001
- Turner, M. A., Yang, X., Yin, D., Kuczera, K., Borchardt, R. T., and Howell, P. L. (2000) *Cell Biochem. Biophys.* **33**, 101–125
- Nagase, T., Ishikawa, K., Suyama, M., Kikuno, R., Hirose, M., Miyajima, N., Tanaka, A., Kotani, H., Nomura, N., and Ohara, O. (1998) *DNA Res.* **5**, 355–364
- Hart, D. N. J. (1997) *Blood* **90**, 3245–3287
- Banchereau, J., and Steinman, R. M. (1998) *Nature* **392**, 245–252
- Ando, H., Mizutani, A., Matsuura, T., and Mikoshiba, K. (2003) *J. Biol. Chem.* **278**, 10602–10612
- Blom, N., Gammeltoft, S., and Brunak, S. (1999) *J. Mol. Biol.* **294**, 1351–1362
- Westerfield, M. (1995) *The Zebrafish Book: Guide for the Laboratory Use of Zebrafish (Danio rerio)*, 3rd Ed., University of Oregon Press, Eugene, OR
- Kimmel, C. B., Ballard, W. W., Kimmel, S. R., Ullmann, B., and Schilling, T. F. (1995) *Dev. Dyn.* **203**, 253–310
- Rupp, R. A., Snider, L., and Weintraub, H. (1994) *Genes Dev.* **8**, 1311–1323
- Westfall, T. A., Hjertso, B., and Slusarski, D. C. (2003) *Dev. Biol.* **259**, 380–391
- Mullins, M. C., Hammerschmidt, M., Kane, D. A., Odenthal, J., Brand, M., van Eeden, F. J., Furutani-Seiki, M., Granato, M., Haffter, P., Heisenberg, C. P., Jiang, Y. J., Kelsh, R. N., and Nusslein-Volhard, C. (1996) *Development* **123**, 81–93
- Berridge, M. J. (1993) *Nature* **361**, 315–325
- Thastrup, O., Cullen, P. J., Drobak, B. K., Hanley, M. R., and Dawson, A. P. (1990) *Proc. Natl. Acad. Sci. U. S. A.* **87**, 2466–2470
- Miller, M. W., Duhl, D. M., Winkes, B. M., Arredondo-Vega, F., Saxon, P. J., Wolff, G. L., Epstein, C. J., Hershfield, M. S., and Barsh, G. S. (1994) *EMBO J.* **13**, 1806–1816
- Baric, I., Fumic, K., Glenn, B., Cuk, M., Schulze, A., Finkelstein, J. D., James, S. J., Mejaski-Bosnjak, V., Pazanin, L., Pogribny, I. P., Rados, M., Sarnavka, V., Scukanec-Spoljar, M., Allen, R. H., Stabler, S., Uzelac, L., Vugrek, O., Wagner, C., Zeisel, S., and Mudd, S. H. (2004) *Proc. Natl. Acad. Sci. U. S. A.* **101**, 4234–4239
- Radomski, N., Kaufmann, C., and Dreyer, C. (1999) *Mol. Biol. Cell* **10**, 4283–4298
- Radomski, N., Barreto, G., Kaufmann, C., Yokoska, J., Mizumoto, K., and Dreyer, C. (2002) *Biochim. Biophys. Acta* **1590**, 93–102
- Mikoshiba, K., Furuichi, T., and Miyawaki, A. (1994) *Semin. Cell Biol.* **5**, 273–281
- Swatton, J. E., Morris, S. A., Wissing, F., and Taylor, C. W. (2001) *Biochem. J.* **359**, 435–441

⁴ M. Kato, K. McDonald, and D. Hart, unpublished results.

Role of AHCYL1 on Zebrafish Development

21. Koulen, P., Janowitz, T., Johnston, L. D., and Ehrlich, B. E. (2000) *J. Neurosci. Res.* **61**, 493–499
22. Nardelli, B., Tiffany, H. L., Bong, G. W., Yourey, P. A., Morahan, D. K., Li, Y., Murphy, P. M., and Alderson, R. F. (1999) *J. Immunol.* **162**, 435–444
23. Koski, G. K., Schwartz, G. N., Weng, D. E., Czerniecki, B. J., Carter, C., Gress, R. E., and Cohen, P. A. (1999) *J. Immunol.* **163**, 82–92
24. Lyakh, L. A., Sanford, M., Chekol, S., Young, H. A., and Roberts, A. B. (2005) *J. Immunol.* **174**, 2061–2070
25. Tenca, C., Merlo, A., Merck, E., Bates, E. E., Saverino, D., Simone, R., Zarcone, D., Trinchieri, G., Grossi, C. E., and Ciccone, E. (2005) *J. Immunol.* **174**, 6757–6763
26. Kume, S., Muto, A., Inoue, T., Suga, K., Okano, H., and Mikoshiba, K. (1997) *Science* **278**, 1940–1943
27. Thrower, E. C., Hagar, R. E., and Ehrlich, B. E. (2001) *Trends Pharmacol. Sci.* **22**, 580–586
28. Devogelaere, B., Nadif Kasri, N., Derua, R., Waelkens, E., Gallewaert, G., Missiaen, L., Parys, J. B., and DeSmedt, H. (2006) *Biochem. Biophys. Res. Commun.* **343**, 49–56

Suppression and Overexpression of Adenosylhomocysteine Hydrolase-like Protein 1 (AHCYL1) Influences Zebrafish Embryo Development: A POSSIBLE ROLE FOR AHCYL1 IN INOSITOL PHOSPHOLIPID SIGNALING

Benjamin J. Cooper, Brian Key, Adrian Carter, Nicola Z. Angel, Derek N. J. Hart and Masato Kato

J. Biol. Chem. 2006, 281:22471-22484.

doi: 10.1074/jbc.M602520200 originally published online June 5, 2006

Access the most updated version of this article at doi: [10.1074/jbc.M602520200](https://doi.org/10.1074/jbc.M602520200)

Alerts:

- [When this article is cited](#)
- [When a correction for this article is posted](#)

[Click here](#) to choose from all of JBC's e-mail alerts

This article cites 27 references, 13 of which can be accessed free at <http://www.jbc.org/content/281/32/22471.full.html#ref-list-1>